Journal of Environmental Management 298 (2021) 113468

Contents lists available at ScienceDirect

Journal of Environmental Management

journal homepage: www.elsevier.com/locate/jenvman

Efficient removal of formaldehyde using metal-biochar derived from acid mine drainage sludge and spent coffee waste

Yongtae Ahn [a], Dong-Wan Cho [b], Waleed Ahmad [a,c], Jungman Jo [a], Jongsoo Jurng [a,c,d], Mayur B. Kurade [e], Byong-Hun Jeon [e], Jaeyoung Choi [a,*]

[a] Center for Environment, Health and Welfare Research, Korea Institute of Science and Technology (KIST), Hwarang-ro 14, Seongbuk-gu, Seoul, 02792, Republic of Korea
[b] Geological Environment Division, Korea Institute of Geoscience and Mineral Resources, 124 Gwahak-ro, Yuseong-gu, Daejeon, 34132, Republic of Korea
[c] Division of Energy and Environment Technology, KIST School, Korea University of Science and Technology (UST), 217 Gajeong-ro, Yuseong-gu, Daejeon, 34113, Republic of Korea
[d] Green School, Korea University, Seoul, Republic of Korea
[e] Department of Earth Resources & Environmental Engineering, Hanyang University, 222-Wangsimni-ro, Seongdong-gu, Seoul, 04763, Republic of Korea

ARTICLE INFO

Keywords:
Spent coffee waste
Metal biochar
Acid mine drainage sludge
Formaldehyde
Adsorption
Fixed column test

ABSTRACT

A novel metal-biochar (Biochar/AMDS) composite were fabricated by co-pyrolysis of spent coffee waste (SCW)/acid mine drainage sludge (AMDS), and their effective application in adsorptive removal of air pollutants such as formaldehyde in indoor environments was evaluated. The physicochemical characteristics of Biochar/AMDS were analyzed using SEM/EDS, XRF, XRD, BET, and FTIR. The characterization results illustrated that Biochar/AMDS had the highly porous structure, carbonaceous layers, and heterogeneous Fe phases (hematite, metallic Fe, and magnetite). The fixed-bed column test showed that the removal of formaldehyde by Biochar/AMDS was 18.4-fold higher than that by metal-free biochar (*i.e.*, SCW-derived biochar). Changing the ratio of AMDS from 1:6 to 1:1 significantly increased the adsorption capacity for formaldehyde from 1008 to 1811 mg/g. In addition, thermal treatment of used adsorbent at 100 °C effectively restored the adsorptive function exhausted during the column test. These results provide new insights into the fabrication of practical, low-cost and ecofriendly sorbent for formaldehyde.

1. Introduction

Formaldehyde is a volatile organic compound (VOC) with irritating odor, which is widely present in daily life and industrial production (Na et al., 2019). Formaldehyde is one of the most commonly detected VOCs of indoor in Korea (Hwang et al., 2018). At ambient temperature, formaldehyde is a colorless, reactive, flammable, and readily polymerized gas. Formaldehyde have detrimental effects on the eyes even at 1 mg/L and it can cause lung cancer under chronic exposure (Lang et al., 2008; Vainio et al., 1994). Formaldehyde is emitted from building materials, decorative materials, furnishings and indoor processes such as heating and cooking (Salthammer et al., 2010). Korean indoor air quality guideline of formaldehyde is regulated below 0.1 mg/L (Environment and Environment, 2020). Several treatment technologies that can reduce formaldehyde in air have been investigated which includes catalytic oxidation, photocatalytic oxidation, phytoremediation, biological degradation, and adsorption (Ji et al., 2020; Carter et al., 2011; Chen et al., 2020; Zhao et al., 2019). When applying photochemical- and biological techniques, a few practical limitations including high operation cost, potential risk in the formation of hazardous by-product, and the delayed reaction time for the treatment restrict their application. On the other hand, adsorption process has been considered as a reasonable method for the removal of formaldehyde because it features high removal efficiency, simple system, easy operation and low cost (Zhang et al., 2017a). Porous materials, which have large surface area, pore volume and functional groups on surface, are widely used for volatile organic compounds (Xiang et al., 2020; Zhang et al., 2017b). Application of coffee waste as biochar raw material for the removal of pollutants is an interesting topic of research (Cho et al., 2015; Zhang et al., 2020; Kim et al., 2018). Coffee is one of the highly consumed beverages in the world and approximately 9.1 million tons of coffee waste was produced in 2016 (Blinová et al., 2017).

* Corresponding author.
E-mail address: jchoi@kist.re.kr (J. Choi).

https://doi.org/10.1016/j.jenvman.2021.113468
Received 24 May 2021; Received in revised form 26 July 2021; Accepted 31 July 2021
Available online 12 August 2021

Yeretzian et al. reported that more than 380,000 brewed coffee waste is disposed every year (Yeretzian et al., 2003). Consequently, coffee waste could be used as raw material for biochar, which is inexpensive and eco-friendly renewable resource (Organization, 2020).

Many researchers reported application of metal-carbon complex in the treatment of VOCs (Jabbari et al., 2016; Pan et al., 2013; Bikshapathi et al., 2012; Amjed et al., 2020). The transitional metal ions loaded on carbon provide additional active adsorption sites or a catalyst initiator, thus metal-carbon complex possess high adsorption capacity of VOCs (Sharif et al., 2021). Several researchers applied acid mine drainage sludge (AMDS) as an adsorbent for heavy metals and organic compounds. The AMDS contains high ratio of iron and aluminum hydroxides, surface structure composed of amorphous micron- and submicron-sized metal oxide/hydroxide particles and has a high specific surface area and numerous functional groups (Cornell and Schwertmann, 2003; Wei and Viadero, 2007). Metal modified biochar showed higher pollutant removal capacity than virgin biochar (Amjed et al., 2020).

Herein, this study developed low-cost and eco-friend adsorbent using industrial by-products and waste material. A novel metal-biochar compositions were fabricated by co-pyrolysis AMDS and spent coffee waste (SCW). However, despite increased the application of biochar as a support material, the usability of metal-biochar as sorbent for the improvement of indoor air quality has been rarely tested yet. The objectives of this research were to synthesize and characterize waste-reclaimed treatment agents from AMDS and coffee waste and evaluate the feasibility of its application to remove formaldehyde. The synthesized biochar/AMDS composition was characterized and the effects of loading dose and initial formaldehyde concentration on the behavior of fixed-bed column was investigated. Reusability of biochar/AMDS composition was also evaluated.

2. Materials and method

2.1. Adsorbent preparation methods

2.1.1. Preparation of metal-biochar precursors and chemicals

AMDS was generated during the operation of active treatment system using $Ca(OH)_2$ as a neutralizing agent. The sludge was collected in the form of bulk solid (>5 cm) from AMD sites in Hamtae mine (Tae-Back city, Gangwon-do, South Korea), screened by a 100-mesh sieve (<150 μm), and then dried at 60 °C for 2 days in an oven prior to use. The coffee waste powder (CW, Brownhouse co., Korea) was provided from a local cafe, Seoul, South Korea. It was screened by a 100-mesh sieve (<150 μm), and then dried at 40 °C for 2 days in an oven prior to use. Thus, the precursors of metal-biochar were prepared in the form of powder to homogeneously mix them for co-pyrolysis in the next section.

2.1.2. Fabrication of metal-biochar

The mixture of CW and AMDS powder were prepared by physically mixing each 3 g of two solids (totally 6 g) without any chemical treatment such as precipitation or wet impregnation. The mixture loaded in an alumina crucible were placed in quartz tube in tubular furnace (GSL-1100X, MTI Co., USA). Co-pyrolysis of two feedstocks was conducted by increasing the temperature from 25 to 800 °C at a heating rate of 10 °C/min until it reached 800 °C where it was maintained constantly during 2 h in N_2 gas-feeding condition (99.99%, 200 mL/min). After cooling the samples, the resulting material (*i.e.*, Biochar/AMDS) was collected using a magnetic stick after the pyrolysis step, and then stored in a desiccator at room temperature. Formaldehyde gas (100 mg/L) and nitrogen gas was purchased from Sinyang Oxygen, Korea.

2.2. Characterization and analytical methods

The chemical constituents of Biochar/AMDS were determined by X-Ray fluorescence spectrometry (XRF) (ZSX Primus II, Rigaku, Japan). To explore the changes in Fe phase of metal-biochar during co-pyrolysis, X-Ray diffractometer (XRD) analysis was conducted using with Cu Kα filtered radiation (Dmax-2500/PC, Rigaku, Japan). The XRD patterns obtained from the analysis were interpreted according to the Joint Committee on Powder Diffraction Standards (JCPDS) in order to provide the mineralogical information. The scanning electron microscopy (SEM) coupled with energy dispersive spectroscopy (EDS) for the elemental analysis using (Inspect F, FEI, USA) were used to compare the surface morphologies of Biochar/AMDS before- and after the adsorption experiments. The Fourier transform infrared (FTIR) spectrophotometer (FT-IR Frontier, PerkinElmer, USA) of adsorbents was analyzed to identify the chemical variation in the surface functional groups before and after the adsorption. The chemical state and electronic state of element on the filter surface of the adsorbents before and after adsorption were characterized by X-ray photoelectron spectroscopy (XPS) (PHI 5000 Versa Probe, ULVAC PHI, Japan). The Brunauer-Emmett-Teller (BET) specific surface area and pore distribution of the adsorbents was measured by N_2 (99.9%) adsorption using a (ASAP 2020, Micromeritics, USA).

2.3. Fixed bed column experiments

The column tests were conducted in a Teflon column of 6 mm internal diameter packed with the adsorbents (Fig. 1). Thick glass wool and glass bead were placed at the bottom of the column to prevent any loss of adsorbent and to give mechanical support to the adsorbent bed. Feeding gas of formaldehyde (10–20 mg/L) and nitrogen (99.9%) was regulated using mass flow controller and in a mixing chamber. The flow rate was controlled at 0.24 L/min. The column experiment was conducted at 30 °C with column oven. The effects of AMDS load dose (0.5, 1.0, and 3.0 g) was investigated. Formaldehyde concentration was quantitatively determined using FTIR (I4001–F, MIDAC Co., USA). The amount adsorbed of the materials (q_e, mg/g) was calculated from following Eq. (1):

$$q_e = \frac{QC_0}{m}\int_{t_0}^{t_s}\left(1-\frac{C}{C_0}\right)dt \quad (1)$$

where Q (L min^{-1}) is the total volumetric flow rate, C_0 (mg/L) is the inlet formaldehyde concentration, C (mg/L) is the outlet formaldehyde concentration, t_0 is initial time, t_s is the saturation time, and m (g) is mass of adsorbent, which is filling into the column.

2.4. Regeneration

The recyclability of the adsorbents was tested through three cycles. The used adsorbent was placed in oven at 80 °C for 1 day to desorb formaldehyde adsorbed during the earlier cycle. Regenerated samples were stored in desiccator for the subsequent cycles.

3. Results and discussion

3.1. Characterization of biochar/AMDS composition

The physical characteristics of the adsorbent including surface area, pore size, and pore volume are summarized in Table 1. Metal-free biochar showed poor porosity (0.001 cm^3/g) and BET surface area (SA) (0.950 m^2/g), indicating the present pyrolysis condition (contact time, temperature, and type of atmospheric gas) failed to produce the hierarchically porous biochar. Whereas, AMDS addition created the porous structure (SA: 64.80 m^2/g, pore volume: 0.096 cm^3/g) in biochar matrix at the same pyrolytic condition, which is consistent with the BET results of previous work showing the increase of porosity by metal-oxide impregnation (Yin et al., 2018). The SEM images and EDX analysis

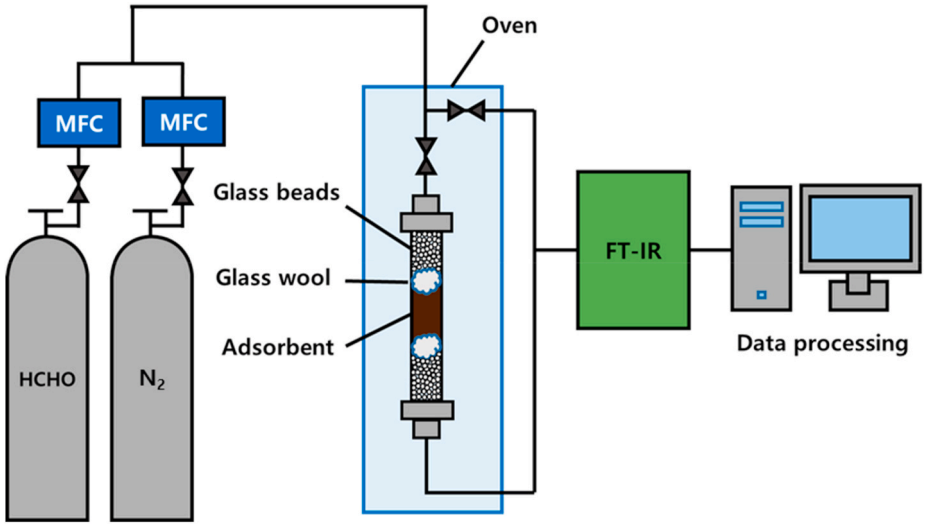

Fig. 1. Experimental set-up.

Table 1
Surface characteristics of adsorbents.

Sample	Surface area (m^2/g)	Pore volume (cm^3/g)	Pore size (nm)
Biochar	0.950	0.001	5.181
Biochar/AMDS	64.796	0.096	5.944

results of biochar and biochar/AMDS composite are presented in Fig. S1. The surface morphologies of biochar showed that it has porous structure containing macro-pores (Fig. S1 (a)). In contrast, the SEM image of the biochar/AMDS showed that macro pore was occupied by some of iron oxide (Fig. S1 (c)). The analysis of EDX was conducted to determine the surface elemental compositions. The EDS spectra results confirmed successful iron oxide modification on surface of biochar/AMDS composition (Fig. S1 (b, d)). The Ca was detected after AMDS impregnation, which might be due to $Ca(OH)_2$ neutralize agent. The major constituents of AMDS, which analyzed by XRF, were Fe_2O_3 (56.6%), CaO (30.2%), SiO_2 (4.6%), and Al_2O_3 (3.6%), reflecting high amounts of iron oxide together with low contents of Ca, Si, and Al (Table 2).

3.2. *Effect of operational parameters on performance of fixed-bed column*

The formaldehyde inlet gas, which diluted with nitrogen gas was introduced into the fixed bed column with flow rate of 0.24 L/min. The performance of formaldehyde removal in column was expressed by the breakthrough curve, which was outlet formaldehyde concentration against the flow time (t). The exhaust point time, which usually called breakthrough point, defined as outlet concentration of formaldehyde reached its 90% of inlet concentration. Some experimental conditions need long duration to reach the bed saturation, therefore, for the performance comparison, the exhaust point time was arbitrarily decided. The formaldehyde removal ability of sorbents decreases as they are gradually saturated with formaldehyde, so the concentration at the outlet increases slowly. As AMDS loading dose increased, the exhaust point time of adsorbent increased from 227 min to 285 min, and the saturation capacity reached to 1811 mg/g, respectively (Fig. 2 (a)). These results indicated that AMDS loading dose play an important role in exhaust point time of adsorbent. Formaldehyde adsorption capacity of Biochar/AMDS was 18.4 fold higher than that of the biochar. Previous researchers applied adsorbent including Granular activated carbon (GAC), zeolite, biochar, and metal organic framework (MOF) for formaldehyde removal (Carter et al., 2011; Kalantarifard et al., 2016; Krishnamurthy et al., 2018). Modification of adsorbent enhanced formaldehyde adsorption capacities, physical modification of activated carbon increased formaldehyde adsorption capacities from 334.7 mg/g (GAC) to 404.3 mg/g (activated carbon fiber). Metal impregnation also increased formaldehyde adsorption capacity of adsorbent, Rengga et al. also reported that silver impregnation increased formaldehyde adsorption capacity to 119.3 mg/g after surface modification. As formaldehyde concentration increased, the exhaust point time of adsorbent reduced from 285 to 129 min, and the saturation capacity reached to 1711 mg/g, respectively (Fig. 2 (b)). High concentration of formaldehyde resulted the exhaust point time significantly decreased.

In order to evaluate adsorption capacity of Biochar/AMDS, comparison of its adsorption capacity for formaldehyde with previously reported adsorbents and results are summarized in Table 3. Chemical modification of zeolite with clinoptilolite also increased formaldehyde adsorption capacities from 106.7 mg/g (zeolite) to 300.5 mg/g (Modified clinoptilolite zeolite). MOF is also an attractive adsorbent, which consist of metal and organic compound. Krishnamurthy applied MIL-101(Cr) to remove formaldehyde, it showed 99.1 mg/g formaldehyde adsorption capacity. While the formaldehyde is passed over the adsorbent, formaldehyde adsorbed onto the adsorbent surface via hydrogen bonding between the H atom of formaldehyde and O atom of adsorbent. The AMDS modification increased surface area and pore volume that might have enhanced formaldehyde adsorption. Biochar/AMDS showed higher surface area and pore volume than Biochar (Table 1). Another possibility is that the presence of positively charged metal atoms or hydroxyl groups on Biochar/AMDS surface, observed in the FT-IR results (Fig. S1), can enhance the adsorption of formaldehyde through strong electrostatic interactions (Yin et al., 2018; Kalantarifard et al., 2016; Krishnamurthy et al., 2018; Carneiro and Cruz, 2008; Xu et al., 2019). Previous researchers (Carneiro and Cruz, 2008; Xu et al., 2019) also observed synergetic adsorption with transition metal via adsorption-oxidation including formaldehyde adsorbed adsorbent

Table 2
XRF analysis of AMDS.

Elements	MgO	Al_2O_3	SiO_2	SO_3	K_2O	CaO	MnO	Fe_2O_3	ZnO	SrO
Chemical composition (%)	0.88	3.63	4.63	0.94	0.18	30.2	2.19	56.6	0.23	0.28

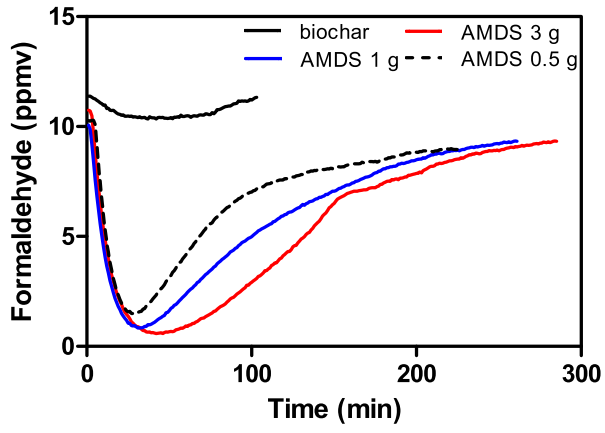

(a)

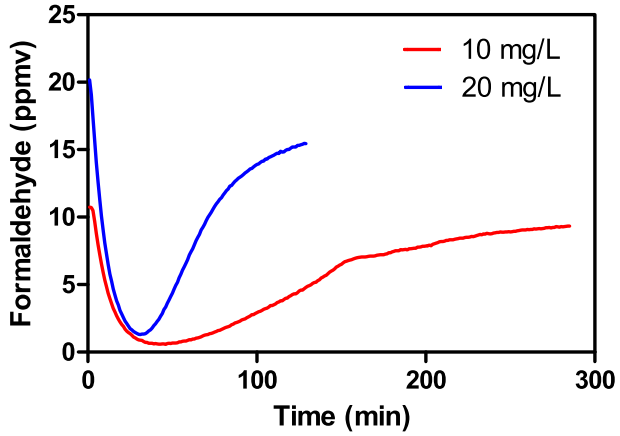

(b)

Fig. 2. Effect of (a) AMDS loading and (b) inlet concentration on formaldehyde removal performance (Flow rate: 0.24 L/min, dose: 0.2 g, room temperature).

surface via hydrogen bonding between the H atom of formaldehyde and O atom of adsorbent. The electrostatic attraction between M^{2+} of adsorbent and O atom of formaldehyde, hydroxyl radicals generated by reaction which adsorbed oxygen interacted with hydroxyl ions nearby the M^{2+}, and active hydroxyl radicals react with adsorbed formaldehyde.

The XRD patterns (Fig. 3) of sample confirmed that the diffraction peaks of 2θ = 43.7 and 51.0° related to carbonized carbon were observed in biochar (Shin et al., 2021). The XRD patterns of AMDS revealed the existence of magnetite (Fe_3O_4), hematite (Fe_2O_3) and goethite. Interestingly, new peaks (2θ = 44.6, 65.0, and 82.3°) were appeared in Biochar/AMDS after co-pyrolysis at 800 °C in N_2, while a few peaks corresponding to goethite (2θ = 20.2, 26.6, 33.1 and 36.2°) were removed instead. These observations can be explained by the reduction of iron oxide to magnetite through the thermochemical reaction (Cho et al., 2019). Hematite (Fe_2O_3) and metallic Fe were found at Biochar/AMDS. Metallic Fe formed via thermal treatment in N_2 at 800 °C (Yoon et al., 2020). The peaks assigned to Hematite and metallic Fe disappeared after formaldehyde adsorption. The functional groups of the adsorbents surface were analyzed using FTIR analysis in range of 400–4000 cm^{-1} (Fig. S2). After AMDS modification Fe–O peaks below 700 cm^{-1} were appeared. The peaks appear at 2900, 2520, and 2220 cm^{-1} after exposing the adsorbent to formaldehyde mixture gas. Peak at

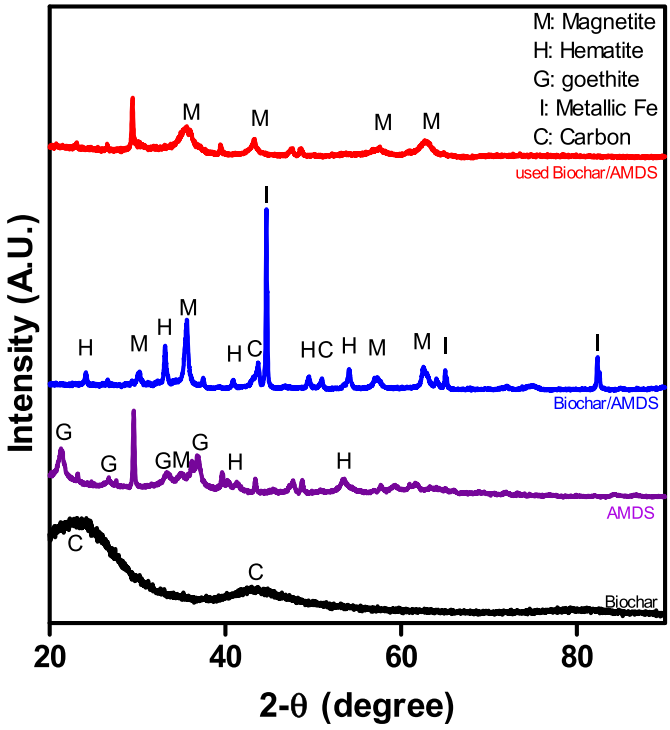

Fig. 3. XRD analysis of Biochar and Biochar/AMDS before and after Formaldehyde adsorption.

Table 3
Comparison of adsorption capacity of biochar/AMDs with pervious reported adsorbents.

Adsorbent	HCHO concentration (ppm)	Experiment condition	Adsorption capacity (mg/g)	Ref.
Granular activated carbon	32.5	Flow rate: 500 mL/min Dose: 0.011 g	334.7	Carter et al., 2011
Siler impregnated activated carbon	1000	Flow rate: 500 mL/min	119.3	Rengga et al., 2017
Activated carbon fiber	32.5	Flow rate: 500 mL/min Dose: 0.011 g	404.3	Carter et al., 2011
zeolite	17.7	Flow rate: 50 mL/min Dose: 0.05 g	106.7	Kalantarifard et al., 2016
Modified clinoptilolite zeolite	17.7	Flow rate: 50 mL/min Dose: 0.05 g	300.5	Kalantarifard et al., 2016
MIL-101(Cr)	170	Flow rate: 40 mL/min Dose: 0.3 g	99.1	Krishnamurthy et al., 2018
Biochar (CW)	13.3	Flow rate: 240 mL/min Dose: 0.2 g	99	This study
Biochar/AMDs	13.3	Flow rate: 240 mL/min Dose: 0.2 g	1074	This study

2900 cm^{-1} corresponds to intermolecular hydrogen bond of the formate (HCOO) conversion from adsorbed formaldehyde at surface site, which is related to the hydrogen bond interactions between Biochar/AMDS and H formaldehyde (Chen et al., 2013). 2520 cm^{-1} corresponds to carboxylic acid OH stretch, 2220 cm^{-1} corresponds to alkyne stretching C≡C. The XPS measurements were performed to explore the elemental information on the surface of Biochar and Biochar/AMDS before and after the adsorption formaldehyde (Fig. 4). Two distinctive peaks were observed at 530.2–530.9 eV and 531.6–532.5 eV in the O 1s spectra of Biochar and Biochar/AMDS before and after the adsorption formaldehyde. The XPS peak at 530.2 eV related to Fe–O bond indicative of Fe_3O_4 (Jiang et al., 2019). Ratio of C–O peak was decreased after AMDS synthetic, while that increased after formaldehyde adsorption. The XPS peak at 531.6 eV corresponded to hydroxyl groups (Kuivila et al., 1988). Five peaks were observed at 710.7–713.5 eV (Fe $2p_{3/2}$), 724.2–727.0 eV (Fe $2p_{1/2}$) and 718.5–718.8 eV (Fe satellite) in Fe 2p spectra of Biochar/AMDS, Tang et al. reported that the Fe $2p_{1/2}$ is tetrahedral coordination and Fe $2p_{3/2}$ is octahedral coordination (Tang et al., 2017). The 711.0 eV and 724.5 eV are characteristic bands of Fe^{3+} from iron oxide (Fe_2O_3) (Kuivila et al., 1988). The 713.5 eV and 727.0 eV are characteristic bands of Fe^{2+} from iron oxide (Fe_3O_4) (Jiang et al., 2019). This observation is consistent with FTIR analysis results of Fe–O peaks.

3.3. Fixed bed adsorption modeling

Fixed-bed column experiment has been widely applied to evaluate adsorbent performance due to easy operation and its high efficiency. Thomas, Adam-Bohart, and Yoon-Nelson models were used to evaluate dynamic behavior of formaldehyde adsorption by adsorbents. These models were well know fixed bed models due to their model equations could be linearized, and then predict its unknown parameters to be estimated via linear regression analysis (Chu, 2020).

The Thomas model used to estimate adsorption capacity of adsorbent and calculate breakthrough curves, assumes that external and internal diffusion constraints were negligible during column test, thus it obey Langmuir isotherm and second-order reversible reaction kinetics (Han et al., 2008). The Thomas model could be represented as below:

$$\ln\left(\frac{C_0}{C_t}-1\right)=\frac{k_{Th}q_e m}{Q}-k_{Th}C_0 t \quad (3)$$

where k_{Th} is Thomas kinetic constant (mL/min mg), t is sample time (min), and Q is flow rate (mL/min), q_e is adsorption capacity of column, C_0 and C_t are inlet and outlet gas concentrations (mg/L). k_{Th} and q_e were determined from plot of C_t/C_0 against t. The column test results were fitted to Thomas model to determine Thomas kinetic constant (k_{Th}) and adsorption capacity of column (q_e). The determined coefficients (R^2) were determined from nonlinear regression (Table 4). As both AMDS loading dose and inlet concentration increased, k_{Th} was increased (from 1.99E-4 to 9.93 E−4 mL/min mg). The value of q_e also increased with AMDS loading dose and inlet concentration (from 23.65 to 35.75 mg/g, and from 35.75 to 37.94 mg/g, respectively). These observations have been reported by the previous researchers (Das et al., 2021; Han et al., 2009). High R^2 values (0.882–0.962) of Thomas model indicated that

Table 4
Parameters of Thomas, Adams-Bohart, and Yoon-Nelson models for adsorption of formaldehyde in fixed-bed column.

Type of model	C_0 (mg L^{-1})	AMDS Loading (g)	Flow rate (L min^{-1})	k_{Th} (mL min^{-1} mg^{-1})	Q_{cal} (mg g^{-1})	R^2
Thomas	10.3	0.5	0.24	4.88E-4	37.91	0.882
	10.1	1.0		8.86 E−4	27.12	0.962
	10.7	3.0		9.01E-4	22.96	0.937
Type of model	**C_0 (mg L^{-1})**	**AMDS Loading (g)**	**Flow rate (L min^{-1})**	**k_{AB} (L mg^{-1} min^{-1})**	**N_{0cal} (mg L^{-1})**	**R^2**
Adam-Bohart	10.3	0.5	0.24	5.726E-4	15.913	0.873
	10.1	1.0		8.598E-4	12.531	0.962
	10.7	3.0		9.862E-4	10.741	0.922
Type of model	**C_0 (mg L^{-1})**	**AMDS Loading (g)**	**Flow rate (L min^{-1})**	**K_{YN} (min^{-1})**	**τ_{cal} (min)**	**R^2**
Yoon-Nelson	10.3	0.5	0.24	0.0165	79.07	0.882
	10.1	1.0		0.0197	115.01	0.962
	10.7	3.0		0.0195	155.48	0.937

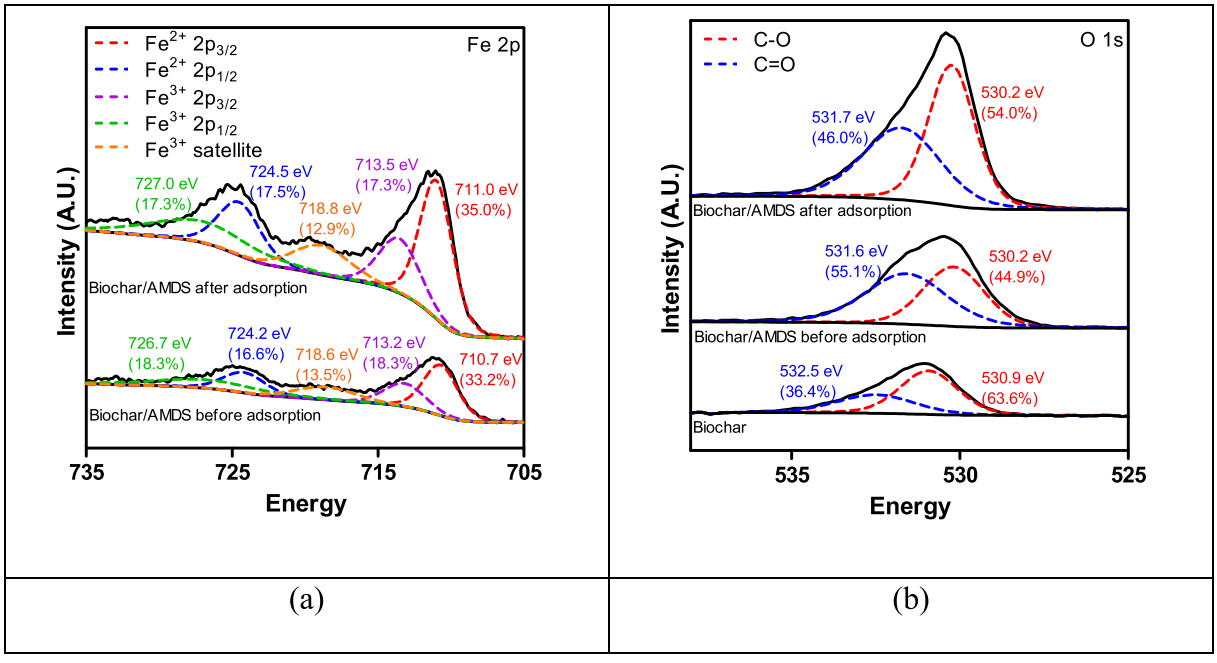

Fig. 4. XPS analysis of Biochar and Biochar/AMDS before and after Formaldehyde adsorption (a) Fe 2p, (b) O 1s.

adsorption between Biochar/AMDS and formaldehyde assumed s Langmuir kinetics and e rate driving force obeys second-order reversible reaction kinetic (Das et al., 2021). As Thomas model is suitable to estimated and predict for adsorption processes, which diffusions between internal and external (Aksu and Gönen, 2004).

Adams and Bohart applied their model for gas-charcoal adsorption system, which showed good agreement in quantitative interfere of similar systems. The Adam-Bohart model assumes that the adsorption rate is proportional to both the residual capacity of the adsorbent and the concentration of the adsorbing species. The Adams–Bohart model is used for the description of the initial part of the breakthrough curve and used to define the breakthrough curve for numerous single-component adsorption systems. Adam-Bohart model focused on estimation of characteristic parameters including saturation concentration (N_0, mg/L) and a kinetic constant (k_{AB}, L/mg). The Adam-Bohart model can be expressed as below:

$$\ln\left(\frac{C_t}{C_0}\right) = k_{AB}C_0 t - k_{AB}N_0\left(\frac{Z}{U_0}\right) \quad (4)$$

where t is the flow time (min), Z is the depth of the fixed-bed column (cm), and U_0 is the superficial velocity (cm/min), C_0 and C_t are inlet and outlet gas concentrations (mg/L). The linear plot of ln (C_t/C_0) against t given the dynamic value of k_{AB}, N_0, and correlation coefficients (R^2). The N_0, k_{AB}, and R^2 were calculated and are summarized in Table 4. The k_{AB} and N_0 increased with AMDS loading dose increased (from 5.64E-4 to 9.83E-4 L/mg min, from 10.78 to 16.04 mg/L, respectively). The value of k_{AB} and N_0 also increased with inlet concentration increasing (from 9.83E-4 to 1.24E-3 L/mg min, from 16.04 to 17.36 mg/L, respectively). These model predictions suggest that the overall kinetics is dominated by external mass transfer (Aksu and Gönen, 2004). These observations have been also reported by previous researchers (Han et al., 2009; Aksu and Gönen, 2004).

The Yoon-Nelson model assume that the decrease in the probability of each adsorbate to be adsorbed is proportional to the probability of its adsorption and breakthrough on the adsorbent (Yoon and Nelson, 1984). Yoon-Nelson model was used to estimate breakthrough performance with single component. The Yoon and Nelson model is simple model compared with other model, it does not need detail information including physical properties of adsorption bed, type of adsorbent, and characteristics of adsorbate. Yoon-Nelson model could be represented as below:

$$\ln\left(\frac{Ct}{C0} - Ct\right) = kYNt - \tau kYN, \quad (2)$$

where τ is time required for 50% adsorbate breakthrough (min), t is flow time (min), k_{YN} is rate constant (min^{-1}), C_0 and C_t are inlet and outlet gas concentrations (mg/L). The dynamic values of k_{YN} and τ were obtained from the linear plot of ln ($C_t/(C_0 - C_t)$) and t (Table 4). k_{YN} increased with AMDS loading dose and inlet concentration increasing (from 6.68E-3 to 1.96E-2/min, from 1.96E-2 to 3.90E-2, respectively). The value of τ decreased with inlet concentration increasing (from 155.67 to 81.67 min). These observations also reported previous researchers (Aksu and Gönen, 2004). Applied three models are well fitted models for formaldehyde adsorption system.

3.4. Reusability of biochar/AMDs composition

Thermal regeneration widely applied to regenerate saturated activated carbon in industry field (Carratalá-Abril et al., 2010). Multi-regeneration study was carried out through adsorption–desorption cycles (Fig. 5). Regeneration conducted as described in chapter 2.4. Regeneration deriving force is heat transfer to emission mechanism (Gu and Bart, 2005). The regeneration rate is defined as Eq. 5

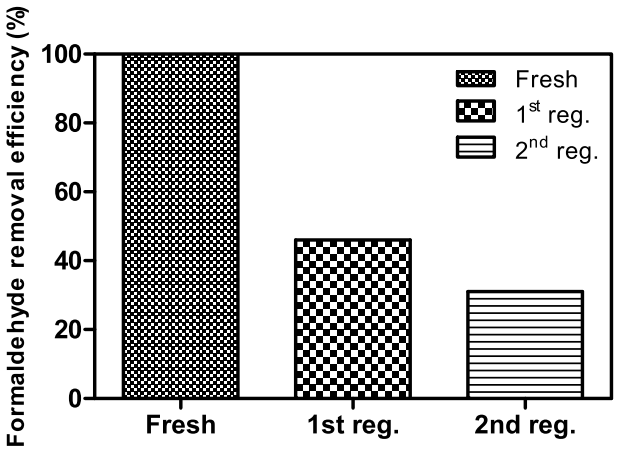

Fig. 5. Biochar/AMDs adsorption performance for formaldehyde after regeneration.

$$r_i = \frac{R_i}{R_0} \quad (5)$$

where r_i is the regeneration ratio of the ith cycle, R_0 and R_i are the fresh and ith regenerated adsorbent's adsorption capacity. The regeneration ratio of Biochar/AMDS reduced as increasing regeneration cycles, to 46% and 31%, respectively. These results indicated that most of the formaldehyde that was adsorbed on the surface of the AMDS had been partially desorbed.

One of possible reason of these phenomena was the reduced surface area with changing pore structure of Biochar/AMDS and changed surface chemistry of AMDS after thermal regeneration (Ledesma et al., 2014). Another possibility is that some of formaldehyde might be adsorbed on the external surface and micropores of the biochar. Adsorbed formaldehyde in micropores might not be desorbed during the low temperature thermal regeneration (Yang et al., 2018). Chen et al also reported that average regeneration rate of formaldehyde adsorbed activated carbon via thermal treatment at 80 °C was about 70%, formaldehyde rapidly desorbed from adsorbent during the regeneration (Chen et al., 2013). The formaldehyde adsorption capacity of adsorbent reduced as it gradually saturated with formaldehyde, thus the outlet formaldehyde concentration increased.

4. Conclusions

In this work, a novel composite, metal-biochar (Biochar/AMDS) was fabricated by one-pot pyrolysis of spent coffee waste and AMD sludge, and its adsorption performance for formaldehyde was examined by conducting the fixed-column experiments. Mixing AMDS with spent coffee waste in pyrolytic process was significantly effective to increase the porosity of biochar. In addition, highly reduced form of Fe oxides (especially metallic Fe) were formed on the surface of biochar via thermal phase transition and the organic constituent substances in coffee waste were also carbonized via dehydrogenation during co-pyrolysis. The column test confirmed that these physicochemical properties of Biochar/AMDS gave the outstanding adsorption function for formaldehyde (1074 mg/g), while biochar only showed the adsorption capacity of 99 mg/g. The exhaust point time was reduced with increasing initial formaldehyde concentration proportionally, while adsorption capacity increased. Biochar/AMDS is a promising adsorbent, which derived from waste materials and highly stable, low-cost material, and demonstrate it could be a practical adsorbent for formaldehyde removal from indoor air. This research is greatly challenging the available formaldehyde adsorbents on the market.

Declaration of competing interest

The authors declare that they have no known competing financial interests or personal relationships that could have appeared to influence the work reported in this paper.

Acknowledgements

This work was supported by the Korea Environment Industry & Technology Institute (KEITI) through the Chemical Accident Prevention Technology Development Project, funded by the Korea Ministry of Environment (MOE) (2020001960001) and the Korea Institute of Science and Technology (Grant 2E29670).

Appendix A. Supplementary data

Supplementary data to this article can be found online at https://doi.org/10.1016/j.jenvman.2021.113468.

Author statement

Yongtae Ahn, Writing – original draft preparation, Methodology, Data curation, Investigation. Dong-Wan Cho, Conceptualization, Writing- Reviewing and Editing. Jungman Jo, Investigation. Waleed Ahmad, Methodology, Investigation. Jongsoo Jurng, Conceptualization. Mayur B Kurade, Writing- Reviewing and Editing. Byong-Hun Jeon, Writing- Reviewing and Editing. Jaeyoung Choi, Supervision, Project administration, Funding acquisition.

References

Aksu, Z., Gönen, F., 2004. Biosorption of phenol by immobilized activated sludge in a continuous packed bed: prediction of breakthrough curves. Process Biochem. 39, 599–613.
Amjed, M.A., Wu, X., Ali, I., Naz, I., Dai, M., Tehrim, A., Niaz, W., Javaid, S.F., Peng, C., 2020. Surface decoration and characterization of solar driven biochar for the removal of toxic aromatic pollutant. J. Chem. Technol. Biotechnol. n/a.
Bikshapathi, M., Singh, S., Bhaduri, B., Mathur, G.N., Sharma, A., Verma, N., 2012. Fe-nanoparticles dispersed carbon micro and nanofibers: surfactant-mediated preparation and application to the removal of gaseous VOCs. Colloid. Surface. Physicochem. Eng. Aspect. 399, 46–55.
Blinová, L., Sirotiak, M., Pastierova, A., Soldán, M., 2017. Review: utilization of waste from coffee production. Res. Pap. Faculty Mater. Sci. Technol. Slovak Univ. Technol. 25.
Carneiro, J.W.d.M., Cruz, M.T.d.M., 2008. Density functional theory study of the adsorption of formaldehyde on Pd4 and on Pd4/γ-Al2O3 clusters. J. Phys. Chem. 112, 8929–8937.
Carratalá-Abril, J., Lillo-Ródenas, M., Linares-Solano, A., Cazorla-Amorós, D., 2010. Regeneration of activated carbons saturated with benzene or toluene using an oxygen-containing atmosphere. Chem. Eng. Sci. 65, 2190–2198.
Carter, E.M., Katz, L.E., Speitel, G.E., Ramirez, D., 2011. Gas-phase formaldehyde adsorption isotherm studies on activated carbon: correlations of adsorption capacity to surface functional group density. Environ. Sci. Technol. 45, 6498–6503.
Chen, D., Qu, Z., Sun, Y., Gao, K., Wang, Y., 2013. Identification of reaction intermediates and mechanism responsible for highly active HCHO oxidation on Ag/MCM-41 catalysts. Appl. Catal. B Environ. 142–143, 838–848.
Chen, M., Wang, H., Chen, X., Wang, F., Qin, X., Zhang, C., He, H., 2020. High-performance of Cu-TiO2 for photocatalytic oxidation of formaldehyde under visible light and the mechanism study. Chem. Eng. J. 390, 124481.
Cho, D.-W., Cho, S.-H., Song, H., Kwon, E.E., 2015. Carbon dioxide assisted sustainability enhancement of pyrolysis of waste biomass: a case study with spent coffee ground. Bioresour. Technol. 189, 1–6.
Cho, D.-W., Yoon, K., Ahn, Y., Sun, Y., Tsang, D.C.W., Hou, D., Ok, Y.S., Song, H., 2019. Fabrication and environmental applications of multifunctional mixed metal-biochar composites (MMBC) from red mud and lignin wastes. J. Hazard Mater. 374, 412–419.
Chu, K.H., 2020. Breakthrough curve analysis by simplistic models of fixed bed adsorption: in defense of the century-old Bohart-Adams model. Chem. Eng. J. 380, 122513.
Cornell, R.M., Schwertmann, U., 2003. The Iron Oxides: Structure, Properties, Reactions, Occurrences and Uses. John Wiley & Sons.
Das, L., Sengupta, S., Das, P., Bhowal, A., Bhattacharjee, C., 2021. Experimental and Numerical modeling on dye adsorption using pyrolyzed mesoporous biochar in Batch and fixed-bed column reactor: isotherm, Thermodynamics. Mass transfer, Kinetic analysis, Surfaces and Interfaces 23, 100985.
Environment, M.o., 2020. In: Environment, M.o. (Ed.), Indoor Air Quality Management Act.
Gu, J., Bart, H.-J., 2005. Heat and mass transfer in steam desorption of an activated carbon adsorber. Int. Commun. Heat Mass Tran. 32, 296–304.
Han, R., Ding, D., Xu, Y., Zou, W., Wang, Y., Li, Y., Zou, L., 2008. Use of rice husk for the adsorption of Congo red from aqueous solution in column mode. Bioresour. Technol. 99, 2938–2946.
Han, R., Wang, Y., Zhao, X., Wang, Y., Xie, F., Cheng, J., Tang, M., 2009. Adsorption of methylene blue by phoenix tree leaf powder in a fixed-bed column: experiments and prediction of breakthrough curves. Desalination 245, 284–297.
Hwang, S.H., Roh, J., Park, W.M., 2018. Evaluation of PM10, CO2, airborne bacteria, TVOCs, and formaldehyde in facilities for susceptible populations in South Korea. Environ. Pollut. 242, 700–708.
Jabbari, V., Veleta, J.M., Zarei-Chaleshtori, M., Gardea-Torresdey, J., Villagrán, D., 2016. Green synthesis of magnetic MOF@GO and MOF@CNT hybrid nanocomposites with high adsorption capacity towards organic pollutants. Chem. Eng. J. 304, 774–783.
Ji, J., Lu, X., Chen, C., He, M., Huang, H., 2020. Potassium-modulated δ-MnO2 as robust catalysts for formaldehyde oxidation at room temperature. Appl. Catal. B Environ. 260, 118210.
Jiang, S.-F., Xi, K.-F., Yang, J., Jiang, H., 2019. Biochar-supported magnetic noble metallic nanoparticles for the fast recovery of excessive reductant during pollutant reduction. Chemosphere 227, 63–71.
Kalantarifard, A., Gon, J., Yang, G., 2016. Formaldehyde adsorption into clinoptilolite zeolite modified with the addition of rich materials and desorption performance using microwave heating. Terr. Atmos. Ocean Sci. 27, 865.
Kim, H.-B., Kim, S.-H., Jeon, E.-K., Kim, D.-H., Tsang, D.C.W., Alessi, D.S., Kwon, E.E., Baek, K., 2018. Effect of dissolved organic carbon from sludge, Rice straw and spent coffee ground biochar on the mobility of arsenic in soil. Sci. Total Environ. 636, 1241–1248.
Krishnamurthy, A., Thakkar, H., Rownaghi, A.A., Rezaei, F., 2018. Adsorptive removal of formaldehyde from air using mixed-metal oxides. Ind. Eng. Chem. Res. 57, 12916–12925.
Kuivila, C.S., Butt, J.B., Stair, P.C., 1988. Characterization of surface species on iron synthesis catalysts by X-ray photoelectron spectroscopy. Appl. Surf. Sci. 32, 99–121.
Lang, I., Bruckner, T., Triebig, G., 2008. Formaldehyde and chemosensory irritation in humans: a controlled human exposure study. Regul. Toxicol. Pharmacol. 50, 23–36.
Ledesma, B., Román, S., Álvarez-Murillo, A., Sabio, E., González, J.F., 2014. Cyclic adsorption/thermal regeneration of activated carbons. J. Anal. Appl. Pyrol. 106, 112–117.
Na, C.-J., Yoo, M.-J., Tsang, D.C.W., Kim, H.W., Kim, K.-H., 2019. High-performance materials for effective sorptive removal of formaldehyde in air. J. Hazard Mater. 366, 452–465.
I.C. Organization, in, 2020.
Pan, H., Tian, M., Zhang, H., Zhang, Y., Lin, Q., 2013. Adsorption and desorption performance of dichloromethane over activated carbons modified by metal ions. J. Chem. Eng. Data 58, 2449–2454.
Rengga, W.D.P., Chafidz, A., Sudibandriyo, M., Nasikin, M., Abasaeed, A.E., 2017. Silver nano-particles deposited on bamboo-based activated carbon for removal of formaldehyde. J. Environ. Chem. Eng. 5, 657–1665.
Salthammer, T., Mentese, S., Marutzky, R., 2010. Formaldehyde in the indoor environment. Chem. Rev. 110, 2536–2572.
Sharif, H.M.A., Mahmood, A., Djellabi, R., Cheng, H.-Y., Dong, H., Ajibade, F.O., Ali, I., Yang, B., Wang, A.-J., 2021. Utilization of electrochemical treatment and surface reconstruction to achieve long lasting catalyst for NOx removal. J. Hazard Mater. 401, 123440.
Shin, J., Lee, Y.-G., Kwak, J., Kim, S., Lee, S.-H., Park, Y., Lee, S.-D., Chon, K., 2021. Adsorption of radioactive strontium by pristine and magnetic biochars derived from spent coffee grounds. J. Environ. Chem. Eng. 9, 105119.
Tang, L., Feng, H., Tang, J., Zeng, G., Deng, Y., Wang, J., Liu, Y., Zhou, Y., 2017. Treatment of arsenic in acid wastewater and river sediment by Fe@Fe2O3 nanobunches: the effect of environmental conditions and reaction mechanism. Water Res. 117, 175–186.
Vainio, H., Heseltine, E., Wilbourn, J., 1994. Priorities for future IARC monographs on the evaluation of carcinogenic risks to humans. Environ. Health Perspect. 102, 590–591.
Wei, X., Viadero Jr., R.C., 2007. Adsorption and precoat filtration studies of synthetic dye removal by acid mine drainage sludge. J. Environ. Eng. 133, 633–640.
Xiang, W., Zhang, X., Chen, K., Fang, J., He, F., Hu, X., Tsang, D.C.W., Ok, Y.S., Gao, B., 2020. Enhanced adsorption performance and governing mechanisms of ball-milled biochar for the removal of volatile organic compounds (VOCs). Chem. Eng. J. 385, 123842.
Xu, Z., Huang, G., Yan, Z., Wang, N., Yue, L., Liu, Q., 2019. Hydroxyapatite-supported low-content Pt catalysts for efficient removal of formaldehyde at room temperature. ACS Omega 4, 21998–22007.
Yang, X., Yi, H., Tang, X., Zhao, S., Yang, Z., Ma, Y., Feng, T., Cui, X., 2018. Behaviors and kinetics of toluene adsorption-desorption on activated carbons with varying pore structure. J. Environ. Sci. 67, 104–114.
Yeretzian, C., Jordan, A., Lindinger, W., 2003. Analysing the headspace of coffee by proton-transfer-reaction mass-spectrometry. Int. J. Mass Spectrom. 223–224, 115–139.
Yin, Q., Wang, R., Zhao, Z., 2018. Application of Mg–Al-modified biochar for simultaneous removal of ammonium, nitrate, and phosphate from eutrophic water. J. Clean. Prod. 176, 230–240.
Yoon, Y.H., Nelson, J.H., 1984. Application of gas adsorption kinetics I. A theoretical model for respirator cartridge service life. Am. Ind. Hyg. Assoc. J. 45, 509–516.

Yoon, K., Cho, D.-W., Bhatnagar, A., Song, H., 2020. Adsorption of As(V) and Ni(II) by Fe-Biochar composite fabricated by co-pyrolysis of orange peel and red mud. Environ. Res. 188, 109809.
Zhang, X., Gao, B., Creamer, A.E., Cao, C., Li, Y., 2017a. Adsorption of VOCs onto engineered carbon materials: a review. J. Hazard Mater. 338, 102–123.
Zhang, X., Gao, B., Zheng, Y., Hu, X., Creamer, A.E., Annable, M.D., Li, Y., 2017b. Biochar for volatile organic compound (VOC) removal: sorption performance and governing mechanisms. Bioresour. Technol. 245, 606–614.
Zhang, X., Zhang, Y., Ngo, H.H., Guo, W., Wen, H., Zhang, D., Li, C., Qi, L., 2020. Characterization and sulfonamide antibiotics adsorption capacity of spent coffee grounds based biochar and hydrochar. Sci. Total Environ. 716, 137015.
Zhao, S., Zhao, Y., Liang, H., Su, Y., 2019. Formaldehyde removal in the air by six plant systems with or without rhizosphere microorganisms. Int. J. Phytoremediation 21, 1296–1304.